Scientific Research Publishing

Advances in Remote Sensing, 2022, 11, 80-105
https://www.scirp.org/journal/ars
ISSN Online: 2169-2688
ISSN Print: 2169-267X

Flood Mapping in Mozambique Using Copernicus Sentinel-2 Satellite Data

Yaw A. Twumasi[1*], Edmund C. Merem[2], John B. Namwamba[1], Abena B. Asare-Ansah[1], Jacob B. Annan[1], Zhu H. Ning[1], Rechael N. D. Armah[1], Caroline Y. Apraku[1], Harriet B. Yeboah[3], Julia Atayi[1], Matilda Anokye[1], Diana B. Frimpong[1], Ronald Okwemba[1], Olipa S. Mwakimi[4], Judith Oppong[1], Brilliant M. Petja[5], Janeth Mjema[1], Priscilla M. Loh[1], Lucinda A. Kangwana[1], Valentine Jeruto[1], Leah Wangari Njeri[1], Joyce McClendon-Peralta[1]

[1]Department of Urban Forestry and Natural Resources, Southern University and A & M College, 102 Fisher Hall, Baton Rouge, Louisiana, USA
[2]Department of Urban and Regional Planning, Jackson State University, 101 Capitol Center, Jackson, Mississippi, USA
[3]Department of Geography and Tourism Studies, Brock University, St. Catharines, Ontario, Canada
[4]Institute of Resource Assessment, University of Dares Salam, Dares Salam, Tanzania
[5]Water Research Commission (WRC) Private Bag X03, Gezina, South Africa
Email: *yaw_twumasi@subr.edu, *yaw.twumasi@gmail.com

How to cite this paper: Twumasi, Y.A., Merem, E.C., Namwamba, J.B., Asare-Ansah, A.B., Annan, J.B., Ning, Z.H., Armah, R.N.D., Apraku, C.Y., Yeboah, H.B., Atayi, J., Anokye, M., Frimpong, D.B., Okwemba, R., Mwakimi, O.S., Oppong, J., Petja, B.M., Mjema, J., Loh, P.M., Kangwana, L.A., Jeruto, V., Njeri, L.W. and McClendon-Peralta, J. (2022) Flood Mapping in Mozambique Using Copernicus Sentinel-2 Satellite Data. *Advances in Remote Sensing*, **11**, 80-105.
https://doi.org/10.4236/ars.2022.113006

Received: November 15, 2021
Accepted: September 27, 2022
Published: September 30, 2022

Abstract

Over the last two decades, Mozambique has experienced tremendous tropical cyclonic activities causing many flooding activities accompanied by disastrous human casualties. Studies that integrate remote sensing, elevation data and coupled with demographic analysis in Mozambique are very limited. This study seeks to fill the void by employing satellite data to map inundation caused by Tropical Cyclones in Mozambique. In pursuit of this objective, Sentinel-2 satellite data was obtained from the United States Geological Survey (USGS)'s Earth Explorer free Online Data Services imagery website covering the months of March 20, 2019, March 25, 2019, and April 16, 2019 for two cities, Maputo and Beira in Mozambique. The images were geometrically corrected to remove, haze, scan lines and speckles, and then referenced to Mozambique ground-based Geographic: Lat/Lon coordinate system and WGS 84 Datum. Data from twelve spectral bands of Sentinel-2 satellite, covering the visible and near infrared sections of the electromagnetic spectrum, were further used in the analysis. In addition, Normalized Difference Water Index (NDWI) within the study area was computed using the green and near infrared bands to highlight water bodies of Sentinel-2 detectors. To project and model the population of Mozambique and see the impact of cyclones on the country, demographic data covering 1980 to 2017 was obtained from the World Bank website. The Exponential Smoothing (ETS) method was adopted to forecast the population of Mozambique. Results from NDWI analysis showed

that the NDWI is higher for flood areas and lower for non-flooded ones. The ETS algorithm results indicate that the population of Mozambique would nearly double by 2047. Human population along the coastal zone in the country is also on the rise exponentially. The paper concludes by outlining policy recommendations in the form of uniform distribution of economic activities across the country and prohibition of inland migration to the coastal areas where tropical cyclonic activities are very high.

Keywords

Tropical Cyclones, Floods, Remote Sensing, NDWI, Exponential Smoothing (ETS), Digital Elevation Model (DEM), Sentinel-2 Satellite, Mozambique

1. Introduction

Tropical cyclones with associated floods are among the major environmental problems facing the world. Cyclones' activities occur from July to September in the Northern Hemisphere and January to March in the Southern Hemisphere [1]. The occurrence of tropical cyclones has been attributed largely to the interaction of warm and cool ocean currents reinforced by high atmospheric pressure [1] [2]. These interactions cause rainfall leading to storm surges. The impacts of flood are prevalent across the globe with intensities occurring in both Northern and Southern Hemispheres as well as Western Hemisphere in the Asian Pacific region. In recent years, tropical cyclones' activities have caused significant impacts on life and property, such as storm surges, flooding, extreme winds, hurricanes, tornadoes, and lightning. In terms of deaths and economic damages associated with tropical cyclones in the United States, Bengtsson [2] noted that during the 2005 hurricane season, including hurricane Katrina, about 1800 lives were lost in New Orleans with damage to property estimated at US$85 billion. According to World Meteorological Organization (WMO), over the past five decades, 1942 disasters have been attributed to tropical cyclones, which has claimed the life of 779,324 people and caused US$ 1407.6 billion in economic losses—an average of 43 deaths and US$ 78 million in damages every day [3]. During a Tropical Cyclone Bhola in 1970 in Bangladesh, between 300,000 and 500,000 people were killed. The tragedy prompted international action and laid the foundation for the WMO Tropical Cyclone Program [3]. Chronology of Atlantic Tropical Cyclones fatalities in the United States has been well documented by Rappaport [4] [5]. According to Rappaport [4] [5] around 2544 people died in the United States or its coastal waters from tropical cyclones in the 50-year period from 1963-2012. He also noted that, the five largest losses, occurred during the Hurricanes Katrina, Camille, Betsy, Agnes, and Sandy with roughly 90% of the deaths occurring through drowning [4] [5] [6]. Further studies conducted by Rappaport and Blanchard [6] investigated whether the fatalities in the United States were indirectly associated with Atlantic Tropical Cyclones and concluded

that from the 59 storms during the 50-year period, the number of direct deaths was 2170 and indirect deaths, 1804 [6].

In the Southeast Asia and the Western Pacific, [7] reviewed historical flood events data from 1980-2009 to determine the impact of cyclones on human populations in terms of mortality, injury, and displacement supported with descriptive statistics and bivariate tests for associations between cyclone characteristics and mortality. Results of the studies revealed there were 412,644 deaths, 290,654 injured, and 466.1 million people affected by cyclones between 1980 and 2009, and the mortality and injury burden were concentrated in less developed nations of Southeast Asia and the Western Pacific [7]. In Japan, Typhoon Hagibis was one the deadliest tropical cyclone to hit the island. The wind originated from West Pacific Ocean and made landfall in Chubu, Kanto, Tohoku regions including Tokyo, from the evening on 12 October 2019 until early morning on 13 October 2019 [8]. According to the published data from the Japanese Red Cross Society (JRCS), with the support of the International Federation of Red Cross and Red Crescent Societies (IFRC), strong wind associated with typhoon caused enormous damages to Japan and resulted in 49 fatalities with 15 people unaccounted for and 234 injured [8]. Over 13,000 houses were partially/destroyed or exposed to water 37,740 houses remain without power and more than 130,000 houses remained without water. This caused more than US$ 15 billion direct economic loss in damages [9]. Other notable Tropical Cyclones such as Maria in 2017 impacted several countries including Dominica, Dominican Republic, Guadeloupe (FRA), Haiti, Martinique (FRA), Puerto Rico, United States of America, Virgin Island (US), and Virgin Island (UK). The losses in Dominica alone totaled to US$ 1.5 billion [9]. Elsewhere in the Greater Antilles (Cuba, Haiti, Dominican Republic, Jamaica, and Puerto Rico), Mexico and Central America, Rappaport [10] reported about 50,000 and 30,000 direct and indirect deaths respectively from the impact of Atlantic Tropical Cyclones. Also, in the Caribbean Sea, Gulf of Mexico, and North Atlantic there were series of tropical cyclone activities in that region in 2016 and 2017. For example, Hurricane Matthew with maximum sustained winds in an excess of 220 km/h, was one of the powerful cyclones that hit Haiti from 3 to 5 October 2016. Hurricane Matthew was accompanied with heavy rains that caused torrential flooding and severe flash floods, mudslides, and landslides [11]. According to the World Meteorological Organization (WMO) thirty-ninth Session's committee report in 2017, an estimated casualty associated with Hurricane Mathew includes 546 dead, 128 unaccounted for and 439 injured, and 2.4 million people were affected. In total, more than 210,000 houses were either destroyed or damaged, and left economic losses amounting to US$ 15.83 billion [9] [11]. Tropical storm Harvey which formed in Barbados, gradually weakened back to a depression early on 19 August 2017, and moved northward and northwestward towards Gulf of Mexico. during the next day or two. Harvey intensified and made a land fall along Texas coast on 24 Harvey which formed in Barbados, gradually weakened back to a depression early on 19 August 2017 at Beaumont-Port Arthur area and south-

western Louisiana at 0800 UTC 30 Harvey which formed in Barbados, gradually weakened back to a depression early on 19 August 2017 near Cameron with 40-kt sustained winds leading to high rainfall which caused flooding. At least 68 people died from the direct effects of the storm in Texas [12].

2. Literature Review of Remote Sensing and GIS of Floods and Flood-Prone Areas

Geospatial information is essential for an effective and quick response to emergency management, especially flooding. GIS and remote sensing technologies play an important role in understanding various disasters, their outcomes, and the damage they could inflict on a given area [13] [14]. Early work by [15] and [16] combined GIS and remote sensing technologies to investigate urban flood zones in Accra, Ghana. Results of the study revealed notable flood risk zones and watercourses. In Southern Mississippi coastal counties, [17] used remote sensing and GIS technology to design an appropriate coastal database in six counties. Results revealed that a greater part of the three counties along the coast lies less than 10 meters above mean sea level with exposure to coastal flooding disaster vulnerability. [18] coupled remote sensing and GIS data to visualize the impact of climate change caused by flooding in the Southern African region to assist decision makers' plans for future occurrences. Result showed the extent of flooded areas. In Louisiana, U.S.A., [19] used satellite remote sensing and Geographic Information System (GIS) data combined with elevation data from the United States Geological Survey (USGS) to identify flood-prone areas in Southeast of Louisiana to help decision-makers develop appropriate adaptation strategies and flood prediction, and mitigation effects on the community. Results of the study revealed that majority of the study area lies in low-lying terrain below sea level. Elsewhere in Queensland, Australia, [20] used NASA's Earth Observing-1 (EO-1) satellite data to identify flooded areas along the roads in the small northern Australian city of Normanton. In Tanjung Selor City, North Kalimantan, Indonesia, [21] employed digital camera fitted on Unmanned Aerial Vehicle (UAV) to identify flood-prone area. In Bihar, India, [22] used Indian remote sensing satellite IRS LISS III, and Landsat TM data to delineate flood-prone areas in the city. Flood risk modeling using remote sensing and GIS has also gained considerable attention. For example, [23] have used remote sensing data to forecast flood hazard. [24] utilized remote sensing techniques combined with Geographic Information Systems-based hydrological modelling to identify flood risk in Ho Chi Minh City, Vietnam. Their study showed that rainfall-induced flood was not a serious problem with the flood depth of 2 - 10 cm while tidal flood was a substantial issue with 10 - 100 cm flood depths [24].

Several studies have employed remote sensing data to assess seasonal floods in Mozambique and neighboring countries [25] [26] [27] [28] [29]. However, none of these studies have integrated remote sensing and elevation data coupled with demographic analysis. This calls for the need to find appropriate methods to aid in identifying floods in Mozambique. Perhaps, the most important element in

these efforts is the need to integrate satellite data with demographics to project and model the population in Mozambique to see the impact of flood on the country. Such information would guide the government to plan better on reducing the loss of human life. The primary objective of this study is to couple elevation, satellite and demographic data to map flood caused by Tropical Cyclones in Mozambique.

3. Methodology

3.1. The Study Area

Mozambique is in the Southern Africa region bordered by the Indian Ocean in the east with Tanzania in the north, Malawi in northwest, Zimbabwe in the west, South Africa in southwest and Eswatini in the south (Figure 1).

Over the last two decades, Mozambique has experienced tremendous tropical cyclonic activities causing many flooding activities accompanied by disastrous human causalities (Figure 2 and Figure 3 and Table 1). Casualty tally from Table 1 shows 1355 deaths related to cyclones in 2019 alone with cyclone Idai being the highest and over 2262 declared missing. The area receives rainfall throughout the year particularly during the winter months. The area lies in the

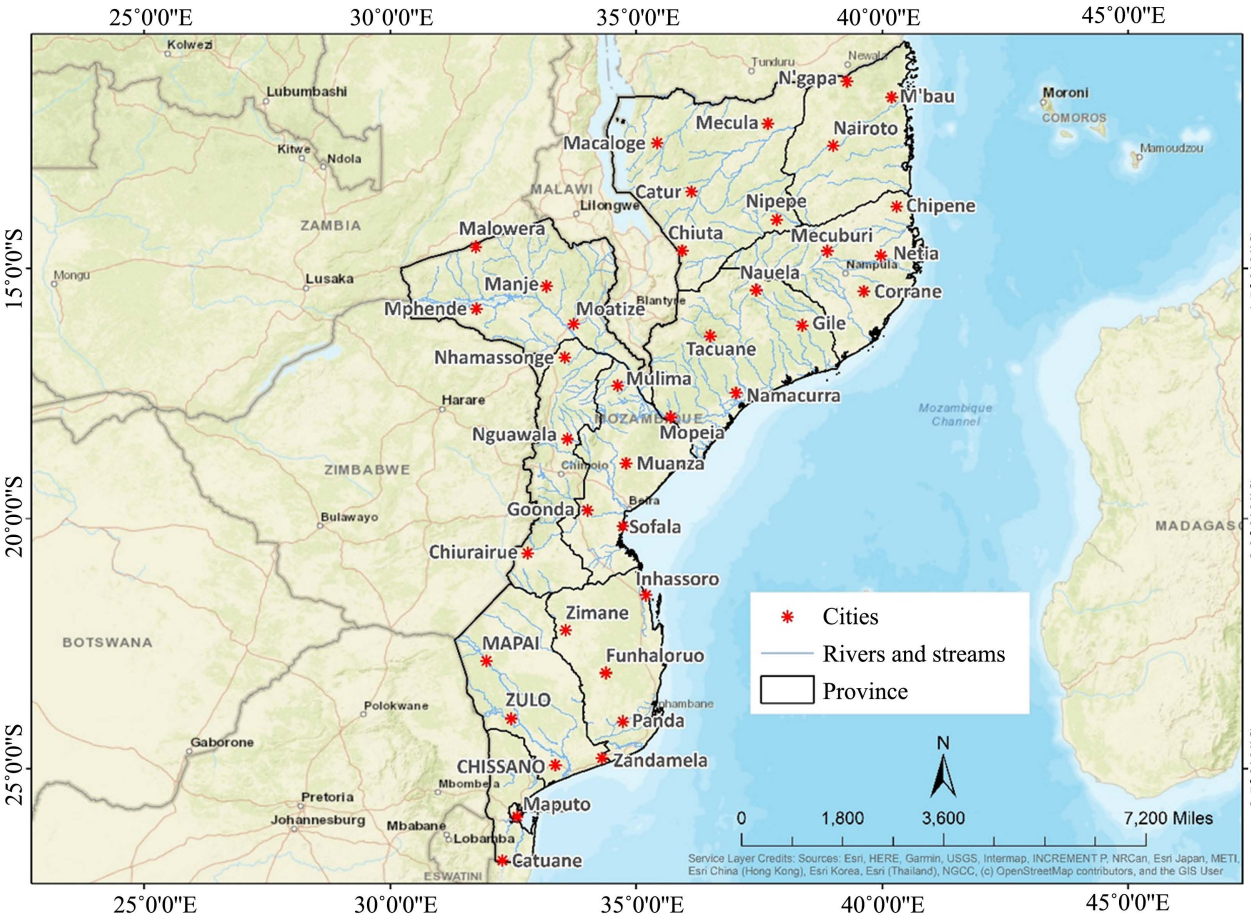

Figure 1. A map showing Mozambique's cities, main towns and provinces [30].

Table 1. Chronology of Selected Major Tropical Cyclones and Their Impacts in Mozambique. Compiled from Wikipedia reference database on Tropical cyclones [33].

Name of Cyclone	Total Death	Win Speed/miles per hr (mph)	Date	Category/ Hurricane	Damage/ $USD
Chalane	7	70	Dec 19, 2020 - Jan 3, 2021	1	Minimal
Idai	≥1303 total ≥2262 missing	127	March 4, 2019 - March 21, 2019	3	2.2 billion
Kenneth	52	143	April 21, 2019 - April 29, 2019	4	100 million
Hellen	8	150	March 27, 2014 - April 1, 2014	4	Unknown
Funso	40	137	January 17, 2012 - January 29, 2012	4	Unknown
Jokwe	16	120	March 2, 2008 - March 16, 2008		8 million
Favio	10	140	11, 2007 - February 23, 2007	4	71 million
Japhet	25	110	25, 2003 - March 6, 2003		None
Elita	33	75	January 26, 2004 - February 5, 2004		
Huda	114	143	22, 2000 - April 9, 2000	4	
Leon-Eline	114 - 722	115	February 1, 2000 - February 29, 2000	4	
Bonita	42	155	January 3, 1996 - January 20, 1996		309 million
Nadia	252	140	March 16, 1994 - April 1, 1994		20.02 million

Figure 2. Track of the tropical cyclone Idai during the 2019 season in Mozambique [31].

equatorial climate region [18]. This is characterized by substantial precipitation ranging between 60 and 180 mm per year. Rainfall is further enhanced by the Sub-Tropical Eastern Continental Moist Maritime System, Inter-tropical Convergence Zone and global weather pattern known as La Niña [18].

Mozambique is the home to numerous major and minor watercourses and basins (**Figure 4**). Major watercourses include Zambezi, Shire, Licungo, Buzi,

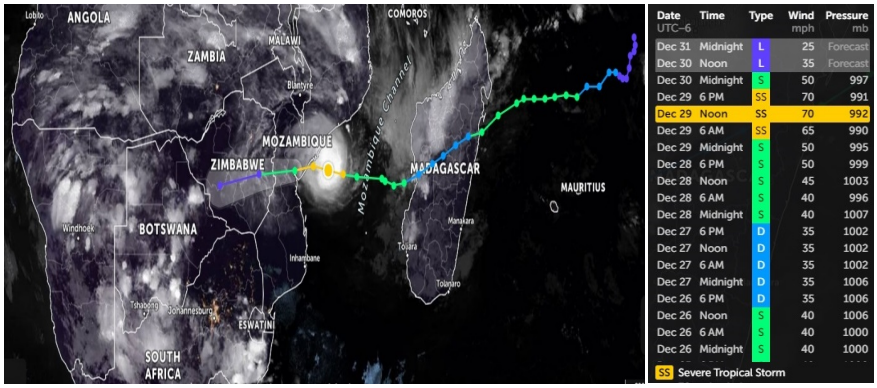

Figure 3. Path of the cyclone Chalane. Photo courtesy of Zoom Earth [32].

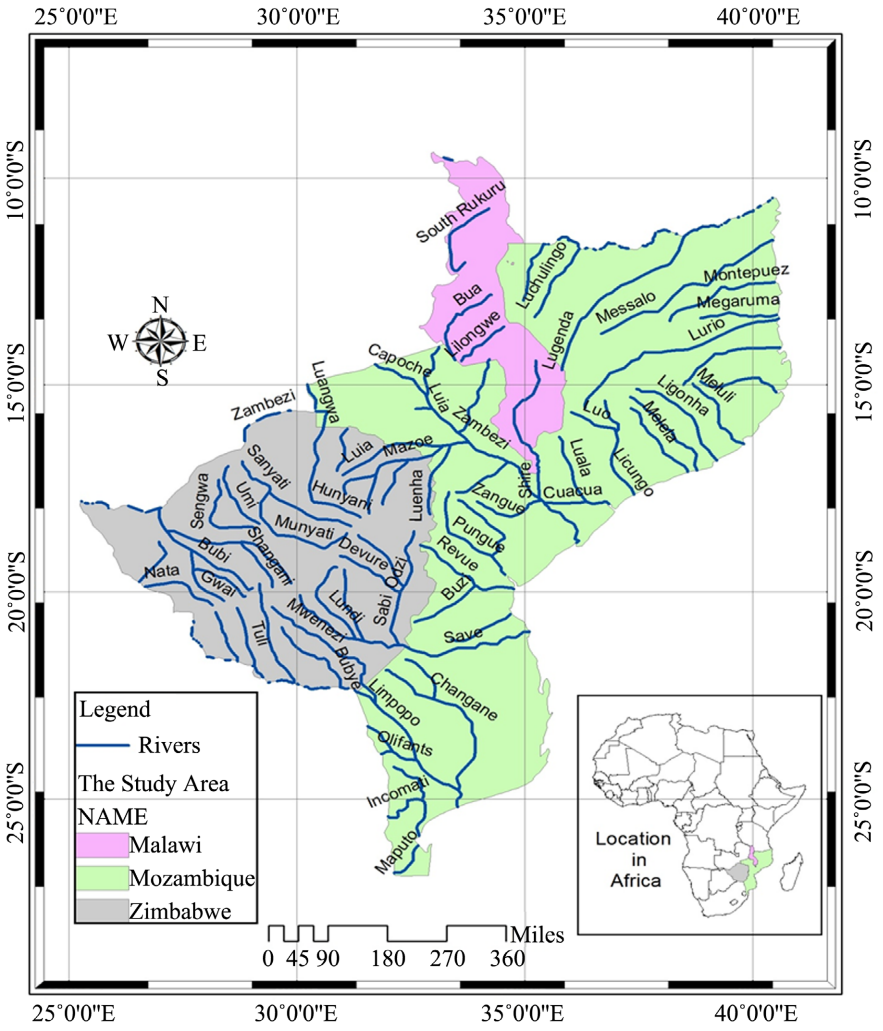

Figure 4. The drainage system in the study area [18].

Save and Limpopo rivers. Many of these watercourses have tributaries which flow into the main river (**Figure 4**). For example, Zambezi River has many tributaries such as Cuacua, Zangue, Shire, Pompue, Luala, Revubue and Luia. In the southwestern part of Mozambique, Limpopo River also has many tributaries.

Some of these include the rivers: Changane, Olifants, Maxim, Chopes, Mwenezi, Babye and Changane. The flow of these two major rivers, Zambezi, and Limpopo, exhibits dendritic patterns to form large watersheds [34].

3.2. Data Acquisition

Sentinel-2 satellite datasets were obtained from the United States Geological Survey (USGS)'s Earth Explorer free Online Data Services imagery website [35]. This consists of Sentinel-2A satellite images acquired on March 20, 2019 for Maputo. Sentinel-2B satellite was also acquired on March 25, 2019, and April 16, 2019 for Beira. The searched areas are shown in **Figure 5** and **Figure 6**. The characteristics of the data acquired for Maputo are shown in **Tables 2-4** below.

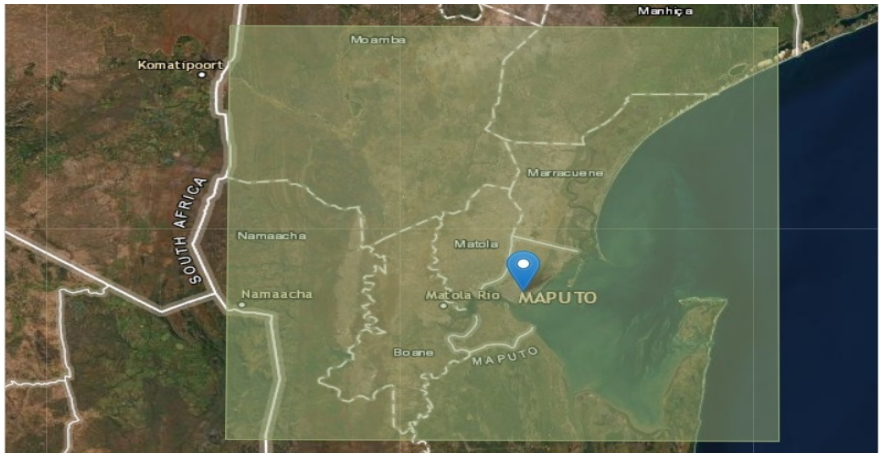

Figure 5. Sentinel-2 satellite data footprint of Maputo.

Figure 6. Sentinel-2 satellite data footprint of Beira.

Table 2. Characteristic of Sentinel-2 data for Maputo.

Image ID	L1C_T36JVS_A019537_20190320T075937
Acquisition Date	2019-03-20T08:07:37.109Z
Tile Number	T36JVS
Cloud Cover	0.00000
Agency	European Space Agency (ESA)
Platform	SENTINEL-2A
Orbit Number	92
Product Format	JPEG2000
Processing Level	LEVEL-1C
Data Type	UINT16
Datum	WGS84
Map Projection	UTM
UTM Zone	36S
Resolution	10, 20, 60
Units	METER

Table 3. Characteristics of Sentinel-2 satellite data for Beira.

Image ID	L1C_T36KXD_A010700_20190325T075425
Acquisition Date	2019-03-25T08:06:59.635Z
Tile Number	T36KXD
Cloud Cover	0.43320
Agency	European Space Agency (ESA)
Platform	SENTINEL-2B
Product Format	JPEG2000
Processing Level	LEVEL-1C
Data Type	UINT16
Datum	WGS84
Map Projection	UTM
UTM Zone	36S
Resolution	10, 20, 60
Units	METER

Table 4. Characteristics of Sentinel -2 satellite data for Beira.

Image ID	L1C_T36KXD_A019923_20190416T074442
Acquisition Date	2019-04-16T07:56:11.526Z

Continued

Tile Number	T36KXD
Cloud Cover	0.99820
Agency	European Space Agency (ESA)
Platform	SENTINEL-2A
Product Format	JPEG2000
Processing Level	LEVEL-1C
Data Type	UINT16
Datum	WGS84
Map Projection	UTM
UTM Zone	36S
Resolution	10, 20, 60
Units	METER

3.3. Image Processing

ERDAS Imagine version 2020 image processing software package was used in this study. The downloaded Images were imported into ERDAS Imagine as a single band using ERDAS native file format jp2000. This was followed by combining all the twelve bands using ERDAS Imagine Layer Stack modules for Maputo and Beira. Since Sentinel-2 imagery has a swath width of 290 kilometers by 290 kilometers, Maputo's image was later subset using ERDAS Imagine Area of Interest Tool (AOI) to emphasize the study area. Data from twelve spectral bands of Sentinel-2, covering the visible and near infrared sections of the electromagnetic spectrum, were further used in the analysis. Normalized Difference Water Index (NDWI) within the study area were computed using the green and near infrared bands to highlight water bodies of Sentinel-2 detectors as proposed by [36]. Sentinel-2 NDWI waterbody detection was constructed by using:

"Green" Band 3 (559 nm) and "NIR" Band 8A (864 nm) ……[37]

NDWI is generally defined as a ratio of the difference to the sum of the intensities of radiation at near infrared and green wavelengths by a satellite sensor, as shown below:

$$NDWI = (B03 - B08)/(B03 + B08)$$

where NDWI represent Normalized Difference Water Index, B03 green band and B08 near-infrared (NIR) band.

3.4. Elevation Data

Elevation data (SRTM/WRS2), covering parts of Southern Africa Region including Mozambique was also obtained from the National Elevation Dataset (NED) produced by the United States Geological Survey (USGS)'s seamless data warehouse. The data was imported into the Global Mapper software version 22

to create the Digital Elevation Model (DEM) surface of Mozambique and the neighboring countries. The idea was to be able to determine the entire elevation of the study area to identify areas that are most susceptible to flooding.

3.5. Population Modeling and Forecasting

To project and model the population in Mozambique to see the impact of cyclones on the country, data covering 1980 to 2017 was obtained from the World Bank website [38]. No missing data was found hence the full data set was used in this research. The data was divided into two parts 1980-2007 as training whiles 2017 was used as a testing data and forecast values generated thereafter. The Exponential Smoothing (ETS) methods were adopted to forecast the population of Mozambique. ETS models are time series models which are part of the family of exponential models which are made up of an error term (E), a trend component (T) and a seasonal component (S).

$$\hat{y}_{n+1|n} = \alpha y_n + (1-\alpha) y_{n-1} + \alpha(1-\alpha) 2 y_{n-2} + \cdots \quad [39] \tag{1}$$

where α, $0 \le \alpha \le 1$, is the smoothing parameter.

ETS (A, N, N)

ETS models with no trends and seasons were used. In ETS it refers to (A, N, N) model. The state space formulation is given as:

$$y_t = y_{t-1} + e_t \quad [39] \tag{2}$$

$$l_t = l_{t-1} + \alpha e_t \quad [39] \tag{3}$$

This formulation can lead to a forecast and smoothing formulation:

$$\hat{y}_{t|t-1} = l_{t-1} \tag{4}$$

$$l_t = \alpha y_{t-1} + (1-\alpha) l_{t-1} \tag{5}$$

where, $\hat{y}_{t|t-1}$ is the forecast of y_t when the previous information is known.

The function FORECAST.ETS in excel was used to generate the forecast population figures in this study [40]. The Syntax for the function is given as;

"=FORECAST.ETS (**target_date, values, timeline, [seasonality], [data_completion], [aggregation**])"

"target_date"—The year being predicted (x value).

"values"—Time series Data points (y values).

"timeline"—Numeric values with constant step interval (x values).

"seasonality"—This argument is optional but deals with Seasonal Component if available in the dataset, 0 signifies absence of seasonality, 1 signifies automatic detection of seasonality whiles *n* signifies specific timeline that seasonality occurs.

"data_completion"—This argument is also optional. It deals with how Missing data are handled (0 = treat as zero, 1 = average).

"Aggregation"—This argument represents Aggregation behavior and optional. For a more detailed discussion on the excel function see [41].

3.6. Results

Result of processed elevation map of Mozambique and the neighboring countries is shown in Figure 7. Figure 8 shows result of Sentinel-2 satellite image covering Southern Mozambique including Maputo. Result of Normalized Difference Water Index (NDWI) image of Southern Mozambique including Maputo is shown in Figure 9. Figure 10 is the NDWI image of Maputo. Figure 11

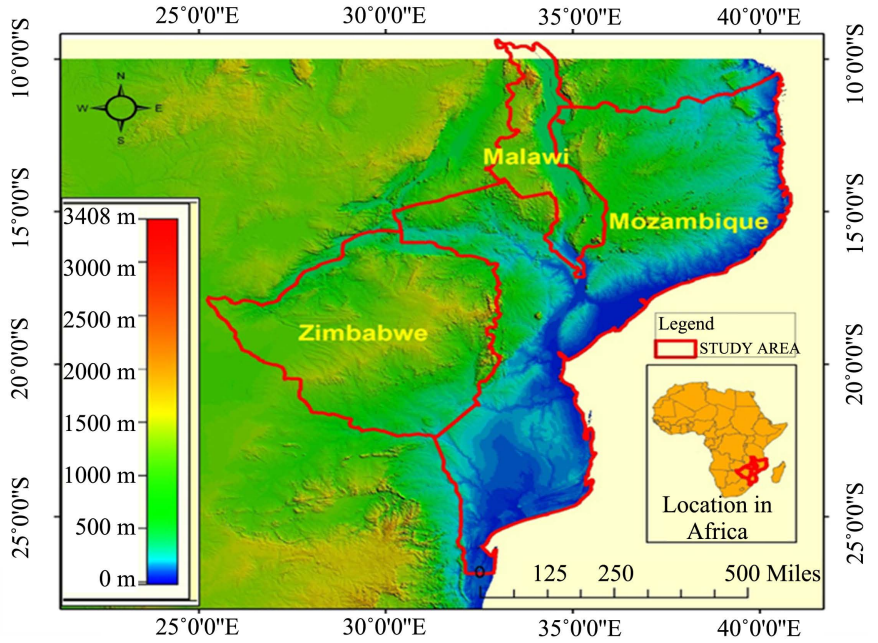

Figure 7. Result of the processed elevation map of Mozambique and the neighboring countries.

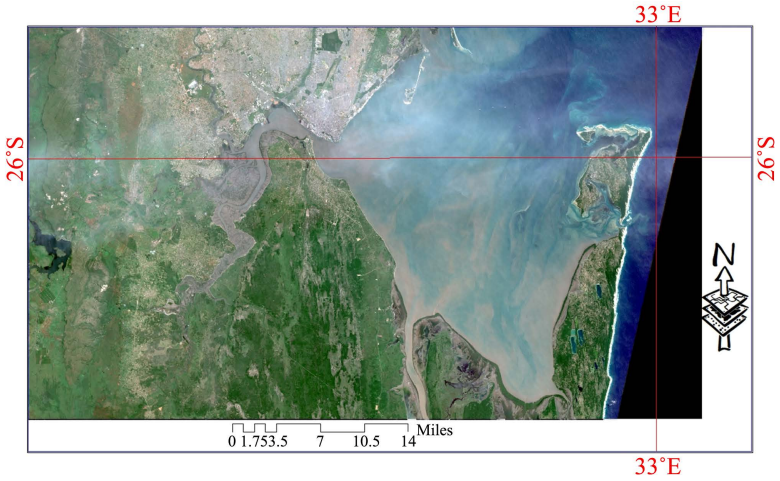

Figure 8. Sentinel -2 satellite Image covering Southern Mozambique including Maputo. The image was captured on March 20, 2019, during Cyclone Idai. This Short-Wave Infrared (SWIR) color composite image was created by combining the red, green, and blue wavelength (bands 12, 8, and 3). Evidence of flooding is captured in the image with color shade of tan representing areas of floods with damages to the vegetation and other cultural features.

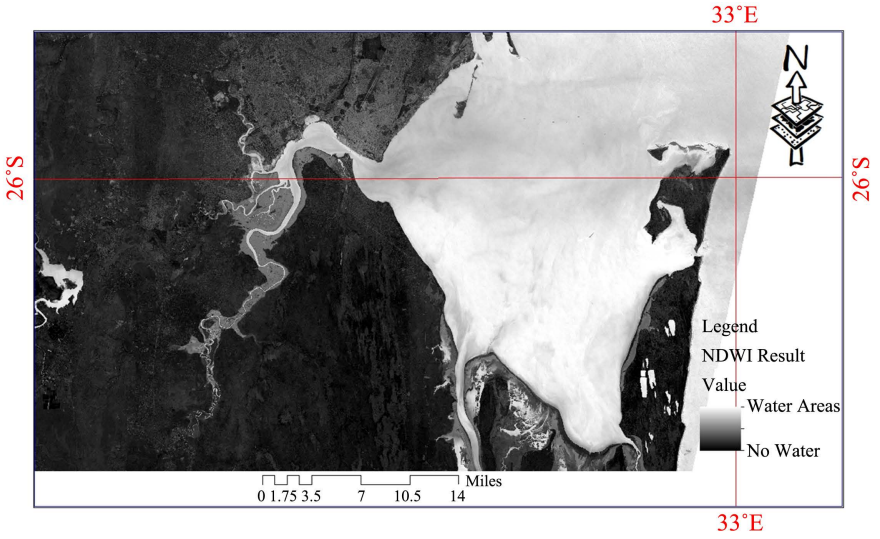

Figure 9. NDWI result of southern mozambique including Maputo.

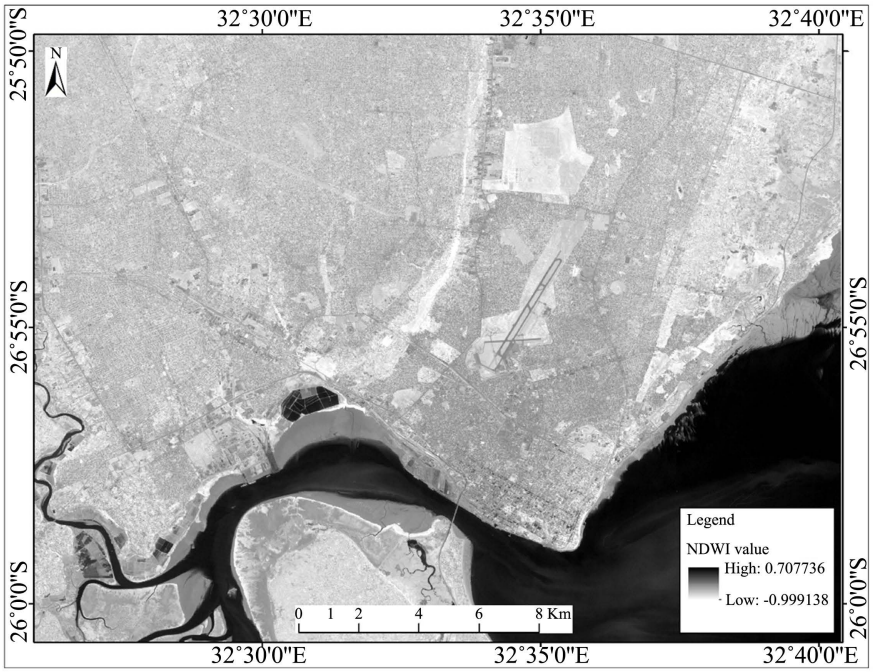

Figure 10. NDWI image of Maputo.

displays the NDWI image of Beira. **Figure 12** shows the NDWI Image of Beira and surrounding areas. Due to low elevation in Mozambique shown in **Figure 7**, most areas get flooded during hurricane and tropical storms. In March and April 2019, Mozambique had two back-to-back tropical cyclones, Idai and Kenneth with devastating combined damages totaling over $2 billion and more than 2000 casualties (**Table 1**); [42]. **Figure 9** shows the impact of cyclone Idai in March 2019. From the image captured by the Sentinel-2 satellite, the eye of the cyclone Idai first hit at Beira as shown in **Figure 2** and **Figure 11**. It dissipated to the south, causing flooding into Maputo and Mozambique Channel (**Figures 8-10**).

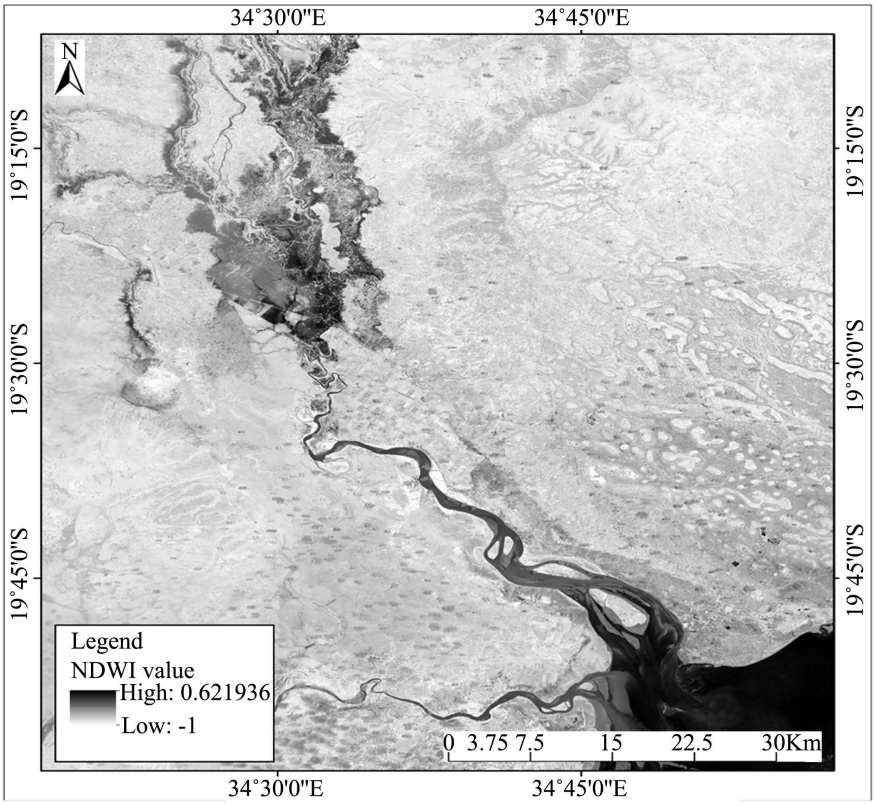

Figure 11. NDWI image of Beira.

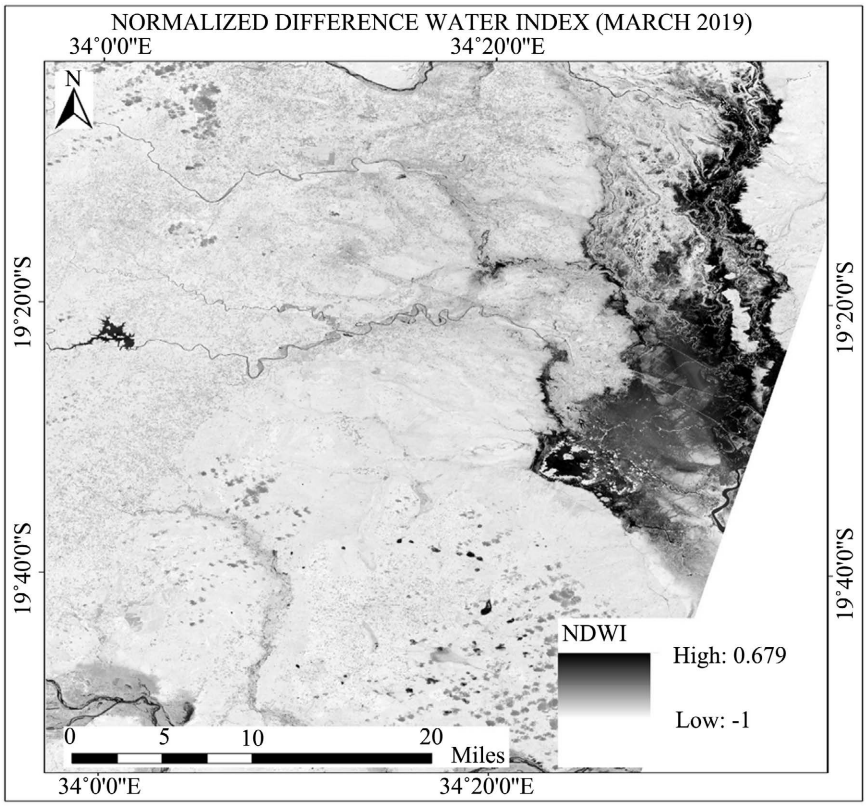

Figure 12. NDWI image of Beira and surrounding areas acquired on March 25, 2021.

3.7. Demographic Analysis

The population of Mozambique for 1980, 1997, 2007 and 2017 which is show in Figures 13-16 were 12,130,000, 16,075,708, 20,632,434, 27,909,799 respectively with 32.53%, 28.35%, 35.27% increase in population for each year. Figure 17 gives information on population of each province in Mozambique. The figure shows that the population of each province is increasing exponentially. Zambézia was the most populous province from 1980 until the 2007 census where Nampula became the most populous province. The least populous province is Maputo Cidade. Maputo saw great increase in population with 68.95% increase from 1980 to 1997, 47.49% increase from 1997 to 2007 and 60.66% increase from 2007 to 2017. There was slight increase in populations at Gaza over the years considered with 12.72% increase from 1980 to 1997, 10.69% increase from 1997 to 2007 and 15.06% increase from 2007 to 2017 as compared to the population increase in all other provinces. The population at Nampula province increased at 27.50% from 1980 to 1997, the province again observed an increase of 33.33% in population from 1997 to 2007 and an exponential increment of 40.99% in population from 2007 to 2017. Generally, the population of each province has adopted an exponential increasing trend. This means the population of the country is increasing rapidly.

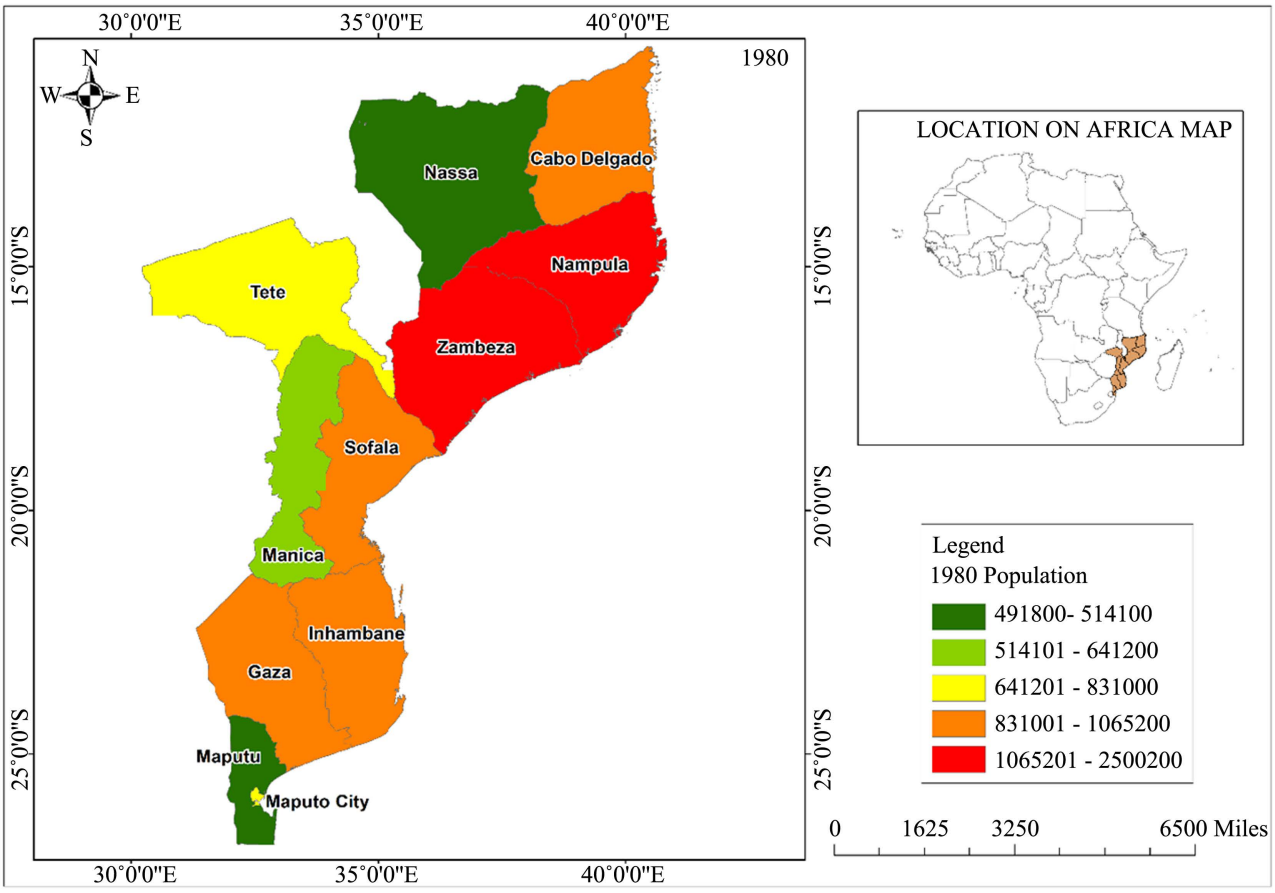

Figure 13. Population of Mozambique in 1980.

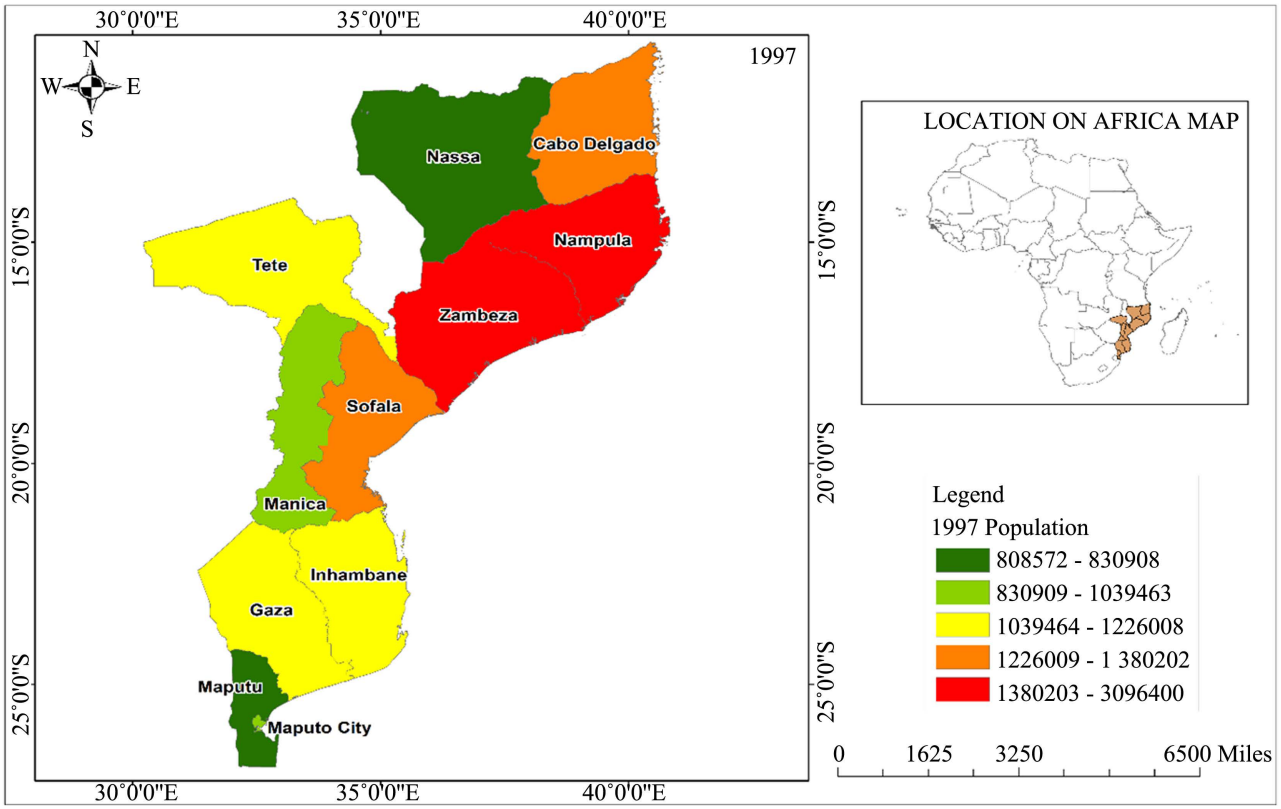

Figure 14. Population of Mozambique in 1997.

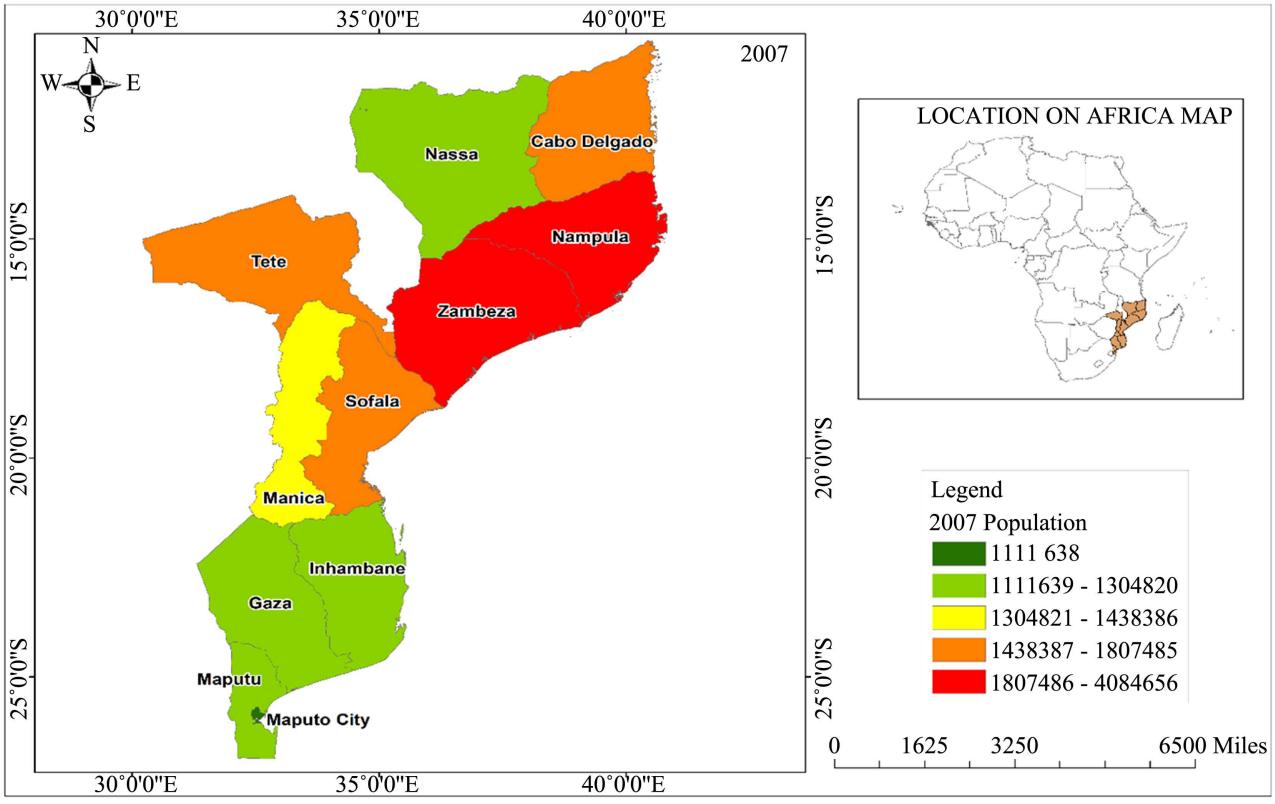

Figure 15. Population of Mozambique in 2007.

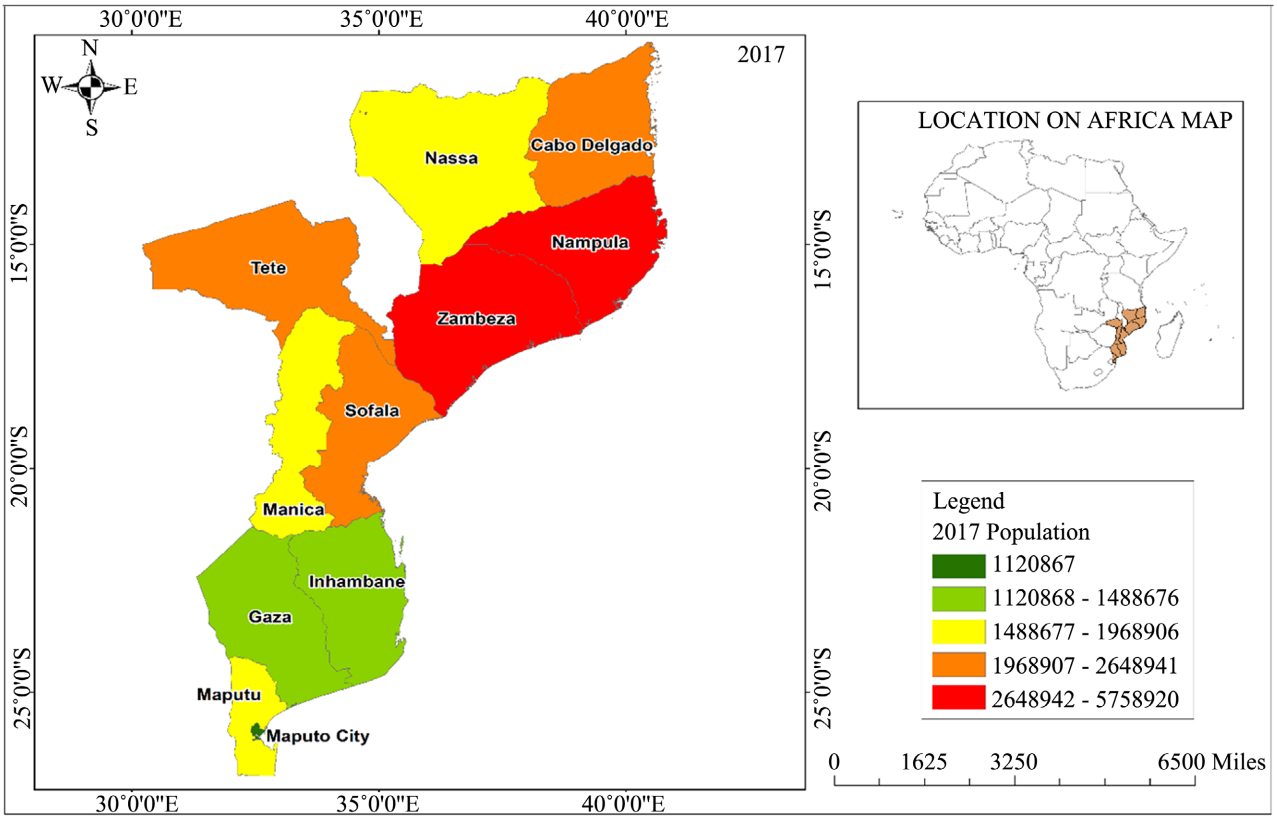

Figure 16. Population of Mozambique in 2017.

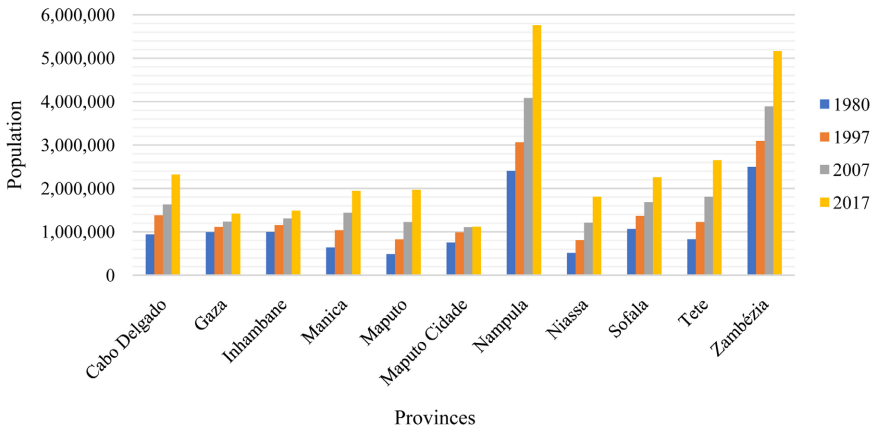

Figure 17. Population of provinces in Mozambique.

3.8. Coastal and Inland Population Analysis

The provinces Cabo Delgado, Gaza, Inhambane, Maputo, Maputo Cidade, Sofala, Nampula and Zambézia are coastal provinces whiles Niassa, Manica, and Tete are not found around the coastal zone. Since majority of the land of Mozambique is found around the coastal zone, most of the population of the country is also centered at the coastal zone as depicted by Figure 18. Despite the established dangers involved in staying at coastal Zones such as flood, cyclonic activities, and excess rainfall [43] [44] [45], population at the coastal zones increases

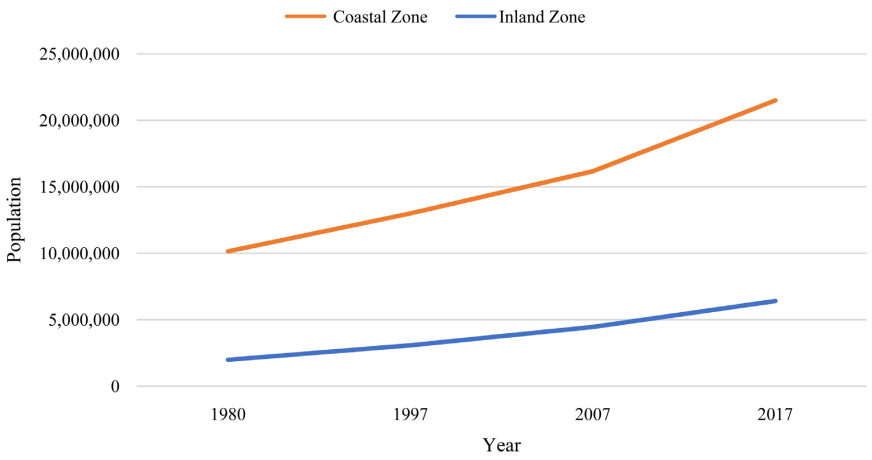

Figure 18. Population of coastal and inland zones in Mozambique.

at a higher rate every year as compared to the inland zones. This increases maybe due to many factors which needs further research to identify them.

3.9. Forecasting Population of the Provinces in Mozambique

3.9.1. Gaza

The forecasted population values for Gaza are 1,422,460 for 2017 with a Lower Limit of 1,422,460 and an upper limit of 1,422,460. The 2027 forecast was 1,496,786 with a Lower Limit of 1,402,449 and an upper limit of 1,591,123. The 2037 forecast was 1,604,714 with a Lower Limit of 1,499,199 and an upper limit of 1,710,228. The population of Gaza has been forecasted to increase gradually from decade to decade, but the increment is not rapid.

3.9.2. Cabo Delgado

The forecasted population values for Cabo Delgado are 2,320,261 for 2017 with Lower Limit of 2,320,261 and upper limit of 2,320,261, 2027 forecast was 2,518,087 with Lower Limit of 2,192,741 and upper limit of 2,843,433, 2037 forecast was 2,851,654 with Lower Limit of 2,516,216 and upper limit of 3,187,091. The forecasted values indicate that the population of Cabo Delgado is increasing exponentially and would eventually be double the figure of 2017 population by 2047 census year.

3.9.3. Inhambane

The Inhambane province is also forecasted to have an increase in population of slightly over 96,000 every ten years. The forecasted population of Inhambane for 2017 is 1,488,676, 2027 is 1,585,273, 2037 is 1,709,365 as shown on Table 5 together with their Upper and Lower Confident Limit. Even though the increase in population is not rapid, it is very significant since the province is having most of its land as Inland with a small portion of it being a coastal zone.

3.9.4. Maputo

Maputo being the Capital of Mozambique, attracts more attention due to its

Table 5. Forecasted population of the Mozambique provinces.

Province	2017			2027			2037		
	Forecast	LCL	UCL	Forecast	LCL	UCL	Forecast	LCL	UCL
Cabo Delgado	2,320,261	2,320,261	2,320,261	2,518,087	2,192,741	2,843,433	2,851,654	2,516,216	3,187,091
Gaza	1,422,460	1,422,460	1,422,460	1,496,786	1,402,449	1,591,123	1,604,714	1,499,199	1,710,228
Inhambane	1,488,676	1,488,676	1,488,676	1,585,273	1,499,803	1,670,744	1,709,365	1,613,768	1,804,962
Maputo	1,968,906	1,968,906	1,968,906	2,177,741	1,746,835	2,608,647	2,544,789	2,062,828	3,026,749
Maputo Cidade	1,120,867	1,120,867	1,120,867	1,248,287	1,175,211	1,321,363	1,343,285	1,267,943	1,418,627
Sofala	2,259,248	2,259,248	2,259,248	2,439,801	2,123,074	2,756,527	2,736,664	2,382,411	3,090,917
Nampula	5,758,920	5,758,920	5,758,920	6,239,961	5,191,284	7,288,637	7,084,261	5,911,335	8,257,186
Zambézia	5,164,732	5,164,732	5,164,732	5,570,176	4,809,998	6,330,354	6,239,746	5,389,501	7,089,991
Niassa	1,810,794	1,810,794	1,810,794	2,017,875	1,659,238	2,376,511	2,345,477	1,944,349	2,746,606
Manica	1,945,994	1,945,994	1,945,994	2,194,470	1,941,540	2,447,399	2,524,505	2,241,608	2,807,401
Tete	2,648,941	2,648,941	2,648,941	2,937,600	2,419,955	3,455,245	3,397,980	2,819,004	3,976,957

economic and agricultural activities. The forecasted population for Maputo is 1,968,906 for 2007, 2,177,741 for 2027, and 2,544,789 for 2037. This trend follows the same trend as the historical population. The forecasted population also indicates that the population of Maputo will be doubled by 2037.

3.9.5. Maputo Cidade

The population of Maputo Cidade has been estimated to be 1,120,867 in 2017 and to reach 1,248,287 by 2027 and 1,343,285 by 2037. The forecasted values indicates that the population of Maputo Cidade is growing gradually but not exponentially and therefore not much pressure would be laid on the resources of the province.

3.9.6. Sofala

Sofala province is also estimated to have population of 2,259,248 by 2017 which exactly as the actual population of the province as 2017 and 2,439,801 by 2027 and finally 2,736,664 by 2037. The population of the province has exponential trend, hence extra pressure would be exerted unto the resources of the province when plans are not made for excess resources for the province.

3.9.7. Nampula

Nampula is the populous province in Mozambique and yet located within the coastal zone and it continues to be even from the forecasted population figures. The forecasted population of Nampula for 2017, 2027 and 2037 are 5,758,920, 6,239,961 and 7,084,261, respectively. The population is deemed to increase with an extreme exponential trend. Here decision makes would need to make plans to contain the extreme growth of the population in the province in other to avoid pressure of sectors of the economy especially on agricultural activities.

3.9.8. Zambézia

Zambézia is the second most populous province in Mozambique and found within the coastal zone. This province like Nampula also continues to increase exponentially in population. The forecasted population for 2017, 2027 and 2037 are 5,164,732, 5,570,176 and 6,239,746, respectively.

3.9.9. Niassa

The province of Niassa is estimated to have an increase around 300,000 every ten years. The forecasted population of Niassa are 1,810,794 for 20,177, 2,017,875 for 2027 and 2,345,477 for 2037. The population forecasted for the province is not exponential and hence when appropriate decisions are taken, there would be no pressure on the resources of the province.

3.9.10. Manica

The forecasted population of Manica for 2017, 2027, and 2037 are 1,945,994, 2,194,470, and 2,524,505, respectively. The population of Manica has also adopted an exponential trend in its growth. Hence the population will increase rapidly with respect to time. Excess pressure would be on the resources of the province if decisions are not taken to counter the growth in population of the province with respect to the resources of the province.

3.9.11. Tete

The population of Tete province has also adopted an exponential trend, the forecasted population also follows the same trend as the actual population of the province. The forecasted population for 2017, 2027, and 2037 are 2,648,941, 2,937,600, and 3,397,980, respectively. As indicated earlier, decision makers would have to consider this growth in population of the province to avoid excess pressure on the resources of the province in the future.

4. Discussions

The results of NDWI analysis from Sentinel-2 satellite data in **Figures 10-12** shows the accumulated inundated areas. According to the images, it implied that the grey color areas had little or no chance of flood within that time of the year. Such areas were not likely to be flooded during the dry season period. The dark color areas have high levels of precipitation and other factors could however increase the chance of flood occurrence during the wet season of the study area. The NDWI also gives a fair idea about the areas that are likely to flood in the event of heavy and continuous rains. From the analysis, areas along the river course, streams and water surfaces are places that are susceptible to floods. Such areas must be evacuated prior to flooding periods to protect life and property. Overall, the NDWI index in **Figures 10-13** revealed the areas covered by surface water for Maputo and Beira. The satellite images confirmed that around that time of the year, there were no flood occurrences. The water surfaces were captured as dark the non-water areas which includes settlements, vegetation and other features of the land appeared in shades of grey. Furthermore, based on

Table 1, the total number of cyclones that have occurred from 1996 to 2019 is 13. Hence, the probability of a cyclone occurring in any given year in future is equal to, 13/25, which is greater than 50%. Hence, the probability of the occurrence of a category 4 cyclone in the event of a cyclone in Mozambique is given as follows.

P (category 4 cyclone/cyclone event) = 6/13 = 46.1%. This implies that in the event of a cyclone in Mozambique, the probability of the cyclone being classified as a category 4 is 46.1%. From the theory of probability, if events A and B are independent, then the probability of both events, A and B occurring is defined as follows.

P (A and B) = P (B ∩ A) = P (B) × P (A) [46]. Hence, the probability of a cyclone of category 4 occurring in any given year in future is equivalent to, the probability of a cyclone occurring and the cyclone being of category 4. Mathematically it is expressed as, Probability of cyclone occurrence) * Probability (category 4 cyclone). P (cyclone occurrence) * P (category 4 cyclone) = (13/25) * 46.1% = 24%, which is almost 25%.

As the population increases in the coastal regions, the number of potential victims of the impacts of the cyclones also increases. The above calculations have just shown that the probability of the next cyclone being of category 4 is quite high, at 46.1%. Hence, the Mozambique government could initiate incentives in the form of investments and employment opportunities to help control the migration. The government could also invest flood safe shelters, emergency transport system, effective and efficient communication systems and well-trained emergency response crews. Although the statistical model employed in this research does not take all factors that affect population into consideration, it predicts future population values well and hence, the forecasted values are reliable**.** Important decisions to reduce the loss of human life and property can therefore be made by both local and international bodies based on the forecasted values in this research.

Analysis and determination of elevations is very important in guiding stakeholders on areas that could be of highest risk to human life and property. Emergency rescue teams can be better trained with the aid of elevation data since it could aid in the design of better life saving drills in preparation of saving human lives when cyclones occur. The possible impacts by cyclones on communities can be felt in the form of loss of lives and livelihood, etc, if the evacuation of the residents is not fast and efficient. To appreciate possible impacts of cyclones in this region, some recent effects of cyclones are presented here. During cyclones people may be faced with danger of drowning, disease, and traumatic experiences. Some of the impacts of various cyclones in Mozambique are presented in Table 1. Among them are, loss of human life, displacement of communities and loss of property. Agricultural land is also destroyed as soil is inundated. An example is Cyclone Ida which inundated and destroyed over 3000 km^2 of agricultural land and displaced around 400,000 inhabitants [28]. Crops on farms that people rely on for food are also destroyed, leading to malnutrition and in-

crease in food insecurity. Whenever there are occurrences of cyclones, food security is also affected, which could lead to starvation among many residents given that many of them depend on their crops for food. Mozambique's National Institute for Disaster Management and Reduction stated that approximately 142,000 hectares of agricultural land were destroyed by cyclone Eloise [47]. This cyclone was a threat to biodiversity and food security. The impacts of flooding on coastal regions of Mozambique are likely to worsen the effects of the rising sea level. The mean sea-level rise for the Mozambican coast is relatively higher than global estimates (~0.05 m) for all representative concentration pathways (RCPs). A rise of the sea level on Mozambican coast was estimated to be between 0.5 and 1.0 m. The impact of cyclones and sea level rise will affect the local population's tourism sector, settlements, and ecosystem services [48].

The damage and loss to the crop sub-sector by one of the cyclones (Ida), was estimated to be about 960.5 million MZN. 38% of the losses were in Manica, 36% in Sofala, 22% in Zambezia and about 3% in Tete province, respectively [49]. These damages were expected to result in losses of income and additional expenditures for the farming households that had been affected and the small, medium, or large farming businesses involved in the production of the cash crops (cotton, tobacco, Cashew, etc.). Apart from the economic loss for direct producers, the different value chains were also expected to incur losses [46]. Following cyclone Idai, over 40,000 families were left without access to safe water in terms of quantity and quality [50].

5. Conclusion

The results indicate clearly that the population of Mozambique will nearly have doubled by 2047. With the exponential population growth in its coastal regions, shown by the results, Mozambique's government needs an appropriate policy that will be focused on dealing with a flooding or other coastal-zone environmental crisis. The rising population in the coastal regions is caused by two factors, population growth through birth and human migration to coastal regions. The former is the greatest contributor. The high rate of population increase in coastal areas reflects the rising number of people at risk of suffering from hurricane related impacts. In this study, Sentinel-2 Satellite Data was successfully used to map the portion of Mozambique flooded following hurricanes. NDWI in flooded areas was found to be higher than in non-flooded areas and higher for flood areas and lower for non-flooded ones. Analysis of the data identified the coastal areas as falling in the region most venerable to impacts of flooding.

Acknowledgements

This work was supported by the United States Department of Agriculture (USDA) National Institute of Food and Agriculture, McIntire Stennis Project NI21MSCFRXXXG003. Also, we would like to extend our sincere gratitude to the Dean of Graduate Studies at Southern University in Baton Rouge, Louisiana,

Professor Ashagre Yigletu for providing graduate assistantships to some of the graduate students on this paper in order to promote research and help the students acquire the necessary skill development while earning a graduate degree.

Conflicts of Interest

The authors declare no conflicts of interest regarding the publication of this paper.

References

[1] Britannica (2020) Location and Patterns of Tropical Cyclones. Encyclopædia Britannica. https://www.britannica.com/science/tropical-cyclone/Location-and-patterns-of-tropical-cyclones

[2] Bengtsson, L. (2007) Tropical Cyclones in a Warmer Climate. WMO *Bulletin*, **56**, 196-202.

[3] World Meteorological Organization (WMO) (2020) 40th Anniversary of the Tropical Cyclone Programme. https://public.wmo.int/en/our-mandate/focus-areas/natural-hazards-and-disaster-risk-reduction/tropical-cyclones/40th_anniversary

[4] Rappaport, E.N. (2000) Loss of Life in the United States Associated with Recent Atlantic Tropical Cyclones. *Bulletin of the American Meteorological Society*, **71**, 2065-2074. https://doi.org/10.1175/1520-0477(2000)081%3C2065:LOLITU%3E2.3.CO;2

[5] Rappaport, E.N. (2014) Fatalities in the United States from Atlantic Tropical Cyclones: New Data and Interpretation. *American Meteorological Society*, **95**, 341-346. https://doi.org/10.1175/BAMS-D-12-00074.1

[6] Rappaport, E.N. and Blanchard, B.W. (2016) Fatalities in the United States Indirectly Associated with Atlantic Tropical Cyclones. *Bulletin of the American Meteorological Society*, **97**, 1139-1148. https://doi.org/10.1175/BAMS-D-15-00042.1

[7] Doocy, S., Dick, A., Daniels, A. and Kirsch, T.D. (2013) The Human Impact of Tropical Cyclones: A Historical Review of Events 1980-2009 and Systematic Literature Review. *PLOS Currents Disasters*, **5**. https://doi.org/10.1371/currents.dis.2664354a5571512063ed29d25ffbce74

[8] OCHA Services Relief Web (2019, October 16) Japan: Typhoon Hagibis - Information Bulletin. https://reliefweb.int/report/japan/japan-typhoon-hagibis-information-bulletin

[9] World Meteorological Organization (WMO) (2020) Notable Tropical Cyclones. https://public.wmo.int/en/our-mandate/focus-areas/natural-hazards-and-disaster-risk-reduction/tropical-cyclones/Notable-tcs

[10] Rappaport, E.N. (2019, May 9) The Causes, Numbers, and locations of Atlantic Tropical Cyclone Fatalities for the 2019 WMO Hurricane Workshop. National Hurricane Center. https://severeweather.wmo.int/TCFW/RAIV_Workshop2019/31_Loss-of-life_EdRappaport.pdf

[11] World Meteorological Organization (WMO) (2017) Reports of Hurricanes, Tropical Storms, Tropical Disturbances and Related Floodings during 2016. *RA IV Hurricane Committee Thirty-Ninth Session*, San Jose, 23-26 March 2017, RA IV/HC-39/Doc. 3.2 (6) (24.II.2017)

https://wmoomm.sharepoint.com/:w:/s/wmocpdb/Efzuw5oVNIpEkG0yDh0SoZQBZMa4Btd_HGeDM1b4Uj8PYQ

[12] World Meteorological Organization (WMO) (2018) 2017 Atlantic and Eastern North Pacific Hurricane Season Summary. *RA IV Hurricane Committee. Fortieth Session*, Fort-De-France, 9-3 April 2018, RA-IV/HC-40/Doc. 3.1 (14.III.2018) https://wmoomm.sharepoint.com/:w:/s/wmocpdb/ESoZBMqRlARKstP9ir-9c_YBPSH4af8_M97WdAqCNoma3Q

[13] Merem, E.C., Twumasi, Y.A., Foster, D., Richardson, C. and Yeramilli, S. (2012) Using GIS and Climate Risks Information to Analyze the Vulnerability of Coastal Counties in Louisiana and Mississippi. *Resources and Environment*, **2**, 1-16. https://doi.org/10.5923/j.re.20120201.01

[14] Mittal, A. (2018) Disaster Management Using Remote Sensing Technology. Sky Map Global. https://skymapglobal.com/disaster-management-remote-sensing/

[15] Twumasi, Y.A. and Asomani-Boateng, R. (2002) Mapping Seasonal Hazards for Flood Management in Accra, Ghana Using GIS. *Proceedings of the IEEE International Geoscience and Remote Sensing Symposium* (*IGARSS*) *Conference*, Toronto, 24-28 June 2002, 2874-2876. https://doi.org/10.1109/IGARSS.2002.1026807

[16] Twumasi, Y.A., Coleman, T.L. and Manu, A. (2003) Integrated Resource Databases for Coastal Zone Management of Metropolitan Accra. *Proceedings of the Annual Convention and Exhibition of the American Society for the Photogrammetry and Remote Sensing* (*ACSM-ASPRS*), Bethesda, 5-9 May 2003, 206-214.

[17] Twumasi, Y.A., Merem, E.C. and Ayala-Silva, T. (2016) Coupling GIS and Remote Sensing Techniques for Coastal Zone Disaster Management: The Case of Southern Mississippi. *Geoenvironmental Disasters*, **3**, Article No. 25. https://doi.org/10.1186/s40677-016-0056-7

[18] Twumasi, Y.A., Merem, E.C., Ayala-Silva, T., Osei, A., Petja, B.M. and Alexander, K. (2017) Techniques of Remote Sensing and GIS as Tools for Visualizing Impact of Climate Change-Induced Flood in Southern African Region. *American Journal of Climate Change*, **6**, 306-327. https://doi.org/10.4236/ajcc.2017.62016

[19] Twumasi, Y.A., Merem, E.C., Namwamba, J.B., Okwemba, R., Ayala-Silva, T., Abdollahi, K., Ben Lukongo, O.E., Tate, J., La Cour-Conant, K. and Akinrinwoye, C.O. (2020) Use of GIS and Remote Sensing Technology as a Decision Support Tool in Flood Disaster Management: The Case of Southeast Louisiana, U.S.A. *Journal of Geographic Information System*, **12**, 141-157. https://doi.org/10.4236/jgis.2020.122009

[20] Riebeek, H. and Gutro, R. (2009, March 16). NASA Satellite Sees Flooding in Queensland, Australia. https://www.nasa.gov/mission_pages/hurricanes/features/queensland_flood.html

[21] Mardiatno, D., Khakim, N. and Priyambodo, T.K. (2015) Identification of Flood-Prone Area Using Remotely Sensed Data—Case in Tanjung Selor City, North Kalimantan. 2015 *IEEE International Conference on Aerospace Electronics and Remote Sensing Technology* (*ICARES*), Bali, 3-5 December 2015, 1-4. https://doi.org/10.1109/ICARES.2015.7429823

[22] Jain, S.K., Singh, R.D. and Jain, M.K. (2005) Delineation of Flood-Prone Areas Using Remote Sensing Techniques. *Water Resource Management*, **19**, 333-347. https://doi.org/10.1007/s11269-005-3281-5

[23] Munawar, H.S., Hammad, A.W.A. and Waller, S.T. (2022) Remote Sensing Methods for Flood Prediction: A Review. *Sensors*, **22**, Article No. 960. https://doi.org/10.3390/s22030960

[24] Dang, A.T.N. and Kumar, L. (2017) Application of Remote Sensing and GIS-Based Hydrological Modelling for Flood Risk Analysis: A Case Study of District 8, Ho Chi Minh City, Vietnam. *Geomatics, Natural Hazards and Risk*, **8**, 1792-1811. https://doi.org/10.1080/19475705.2017.1388853

[25] Allen, J. and Simmon, R. (2013, January 30) Close-Up of Flooding in Mozambique. NASA Earth Observatory. http://earthobservatory.nasa.gov/IOTD/view.php?id=80297

[26] Gray, E. (2015, July 22) Satellite-Based Flood Monitoring Central to Relief Agencies' Disaster Response. NASA's Earth Science News Team. https://www.nasa.gov/feature/goddard/satellite-based-flood-monitoring-central-to-relief-agencies-disaster-response

[27] Carlowicz, M. (2019, April 24) Mozambique Braces for Tropical Cyclone Kenneth. NASA Earth Observatory. https://earthobservatory.nasa.gov/images/144899/mozambique-braces-for-tropical-cyclone-kenneth?src=eoa-iotd

[28] Charrua, A.B., Padmanaban, R., Cabral, P., Bandeira, S. and Romeiras, M.M. (2021) Impacts of the Tropical Cyclone Idai in Mozambique: A Multi-Temporal Landsat Satellite Imagery Analysis. *Remote Sensing*, **13**, Article No. 201. https://doi.org/10.3390/rs13020201

[29] Kettner, A. and Brakenridge, R. (2021, January 25) DFO Flood Event: 2021-Mozambique-5015. DFO Flood Observatory. http://floodobservatory.colorado.edu/Events/5015/2021Mozambique5015.html

[30] World Population Review (2022) Mozambique Population 2022 (Live). https://worldpopulationreview.com/countries/mozambique-population

[31] Ferrell, J. (2019, March 11) Mozambique Hurricane History vs. Cyclone Idai. https://www.accuweather.com/en/weather-blogs/weathermatrix/mozambique-hurricane-history-vs-cyclone-idai/596

[32] Zoom Earth (2020) Satellite Images and Tracking Maps of Tropical Storm Chalane 2020. https://zoom.earth/storms/chalane-2020/

[33] Wikipedia (2022) Tropical Cyclones in Southern Africa. https://en.wikipedia.org/wiki/Tropical_cyclones_in_Southern_Africa

[34] Sarker, S., Veremyev, A., Boginski, V. and Singh, A. (2019) Critical Nodes in River Networks. *Scientific Reports*, **9**, Article No. 11178. https://doi.org/10.1038/s41598-019-47292-4

[35] U.S. Geological Survey (2020) EarthExplorer-Home. Satellite Data. https://earthexplorer.usgs.gov/

[36] McFeeters, S.K. (1996) The Use of the Normalized Difference Water Index (NDWI) in the Delineation of Open Water Features. *International Journal of Remote Sensing*, **17**, 1425-1432. https://doi.org/10.1080/01431169608948714

[37] Wikipedia (2020) Normalized Difference Water Index. https://en.wikipedia.org/wiki/Normalized_difference_water_index

[38] The World Bank (2020) Mozambique Data. https://data.worldbank.org/country/mozambique

[39] Gass, S.I. and Harris, C.M. (2001) Encyclopedia of Operations Research and Management Science: Centennial Edition. Springer Science and Business Media, New York. https://doi.org/10.1007/1-4020-0611-X

[40] Bruns, D. (2019) Excel FORECAST.ETS Function. https://exceljet.net/excel-functions/excel-forecast.ets-function

[41] Microsoft (2021) Worksheet Function.Aggregate Method (Excel). https://docs.microsoft.com/en-us/office/vba/api/excel.worksheetfunction.aggregate

[42] Bevacqua, E., Maraun, D., Vousdoukas, M. I., Voukouvalas, E., Vrac, M., Mentaschi, L. and Widmann, M. (2019) Higher Probability of Compound Flooding from Precipitation and Storm Surge in Europe under Anthropogenic Climate Change. *Science Advances*, **5**, eaaw5531. https://doi.org/10.1126/sciadv.aaw5531

[43] Tobin, G.A. (1997) Natural Hazards: Explanation and Integration. Guilford Press, New York.

[44] Zehra, D., Mbatha, S., Campos, L.C., Queface, A., Beleza, A., Cavoli, C. and Parikh, P. (2019) Rapid Flood Risk Assessment of Informal Urban Settlements in Maputo, Mozambique: The Case of Maxaquene A. *International Journal of Disaster Risk Reduction*, **40**, Article ID: 101270. https://doi.org/10.1016/j.ijdrr.2019.101270

[45] OCHA Services Relief Web (2021, January 29) Mozambique: Tropical Cyclone Eloise - Emergency Appeal N° MDRMZ016. https://reliefweb.int/report/mozambique/mozambique-tropical-cyclone-eloise-emergency-appeal-n-mdrmz016

[46] Palin, P.J., Hanson, L.S., Barton, D. and Frowein, A. (2018) Supply Chain Resilience and 2017 Hurricane Season. CNA Corporation, Arlington County, IRM-2018-U-018098. https://www.cna.org/cna_files/pdf/IRM-2018-U-018098-Final.pdf

[47] Mucova, S.A.R., Azeiteiro, U.M., Lopes, C.L., Dias, J.M. and Pereira, M.J. (2021) Approaching Sea-Level Rise (SLR) Change: Strengthening Local Responses to Sea-Level Rise and Coping with Climate Change in Northern Mozambique. *Journal of Marine Science and Engineering*, **9**, Article No. 205. https://doi.org/10.3390/jmse9020205

[48] Grinstead, C.M., Peterson, W.P. and Snell, J.L. (2012) Probability Tales. American Mathematical Society, Providence. https://doi.org/10.1090/stml/057

[49] Trujillo, M. (2019) Mozambique Cyclone Idai Post-Disaster Needs Assessment (PDNA).

[50] International Committee of the Red Cross (ICRC) (2019) Cyclone Idai: Facts and Figures. https://www.icrc.org/en/document/cyclone-idai-facts-and-figures-0